We are IntechOpen, the world's leading publisher of Open Access books Built by scientists, for scientists

4,800
Open access books available

122,000
International authors and editors

135M
Downloads

Our authors are among the

154
Countries delivered to

TOP 1%
most cited scientists

12.2%
Contributors from top 500 universities

CLARIVATE ANALYTICS BOOK CITATION INDEX INDEXED

WEB OF SCIENCE™

Selection of our books indexed in the Book Citation Index in Web of Science™ Core Collection (BKCI)

Interested in publishing with us?
Contact book.department@intechopen.com

Numbers displayed above are based on latest data collected.
For more information visit www.intechopen.com

Chapter 7

Ultra-Wideband Antenna and Design

Xian Ling Liang

Additional information is available at the end of the chapter

http://dx.doi.org/10.5772/47805

1. Introduction

Ultra-wideband (UWB) antennas are gaining prominence and becoming very attractive in modern and future wireless communication systems, mainly due to two factors. Firstly, people increasingly high demand for the wireless transmission rate and UWB properties such as high data rate, low power consumption and low cost, which give a huge boost to the UWB antennas' research and development in industry and academia since the Federal Communications Commission (FCC) officially released the regulation for UWB technology in 2002. Secondly, now the wireless portable device need antenna operated in different frequencies for various wireless transmission functions, and operation bands and functions are increasing more and more, which may result in challenges in antenna design, such as antenna space limitation, multi antennas interference, and etc. One UWB antenna can be used to replace multi narrow-band antennas, which may effectively reduce the antenna number.

The bandwidth is the antenna operating frequency band within which the antenna performances, such as input impedance, radiation pattern, gain, efficiency, and etc., are desired. The most commonly used definitions for the antenna bandwidth are the fractional bandwidth (for narrow or wideband definition) and the bandwidth ratio (for ultra-wideband definition).

The fractional bandwidth is defined as

$$BW = \frac{f_h - f_l}{f_c} \times 100\% \tag{1}$$

The bandwidth ratio is defined as

$$BW = \frac{f_h}{f_l} : 1 \tag{2}$$

f_l – the lower frequency of the operation band.
f_h – the higher frequency of the operation band.
f_c – the center frequency of the operation band.

2. History of UWB antennas

In 1898, Oliver Lodge [1] firstly introduced the concept of UWB antenna design, such as spherical dipoles, square plate dipoles, triangular or "bow-tie" dipoles, and biconical dipoles. Fig.1 depicts Lodge's biconical antennas which are unmistakenly used in transmit-receive links. After that, a number of types of UWB antennas were developed in the following several years [2-7]. *i.e.*, one of interest rediscoveries of the biconical antenna and conical monopole is done by P. S. Carter in 1939 [2] (See Fig.2). Carter improved upon Lodge's original design by incorporating a tapered feed, one of the key steps towards the design of broadband antennas.

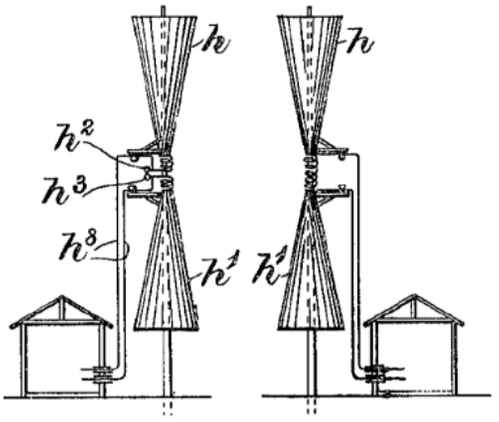

Figure 1. Lodge's biconical antennas (1898).

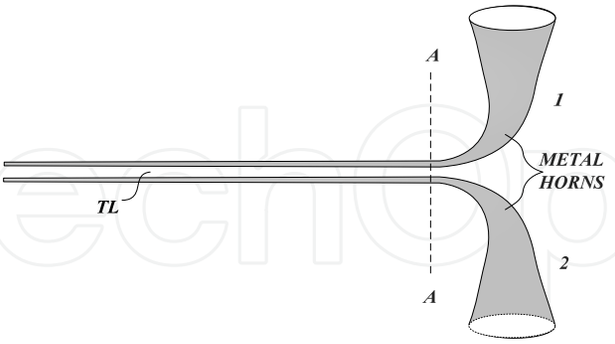

Figure 2. Carter's improved match biconical (1939).

In 1940, S. A. Schelkunoff [3] proposed elaborate conical waveguides and feed structures in conjunction with a spherical dipole (see Fig.3). Unfortunately, his design of the spherical dipole antenna was not very useful. Almost at that time, the most well-known UWB antenna was the coaxial horn proposed by N. E. Lindenblad [4]. In order to make the antenna more broadband, Lindenblad took the design of a sleeve dipole and introduced a continued impedance change, as shown in Fig.4.

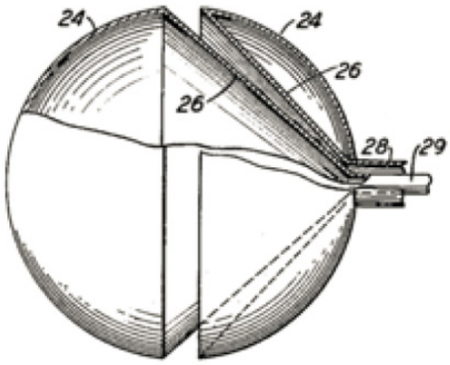

Figure 3. Schelkunoff's spherical dipole (1940)

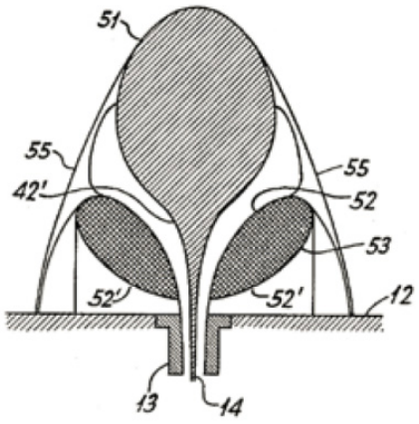

Figure 4. Lindenblad's coaxial horn (1941).

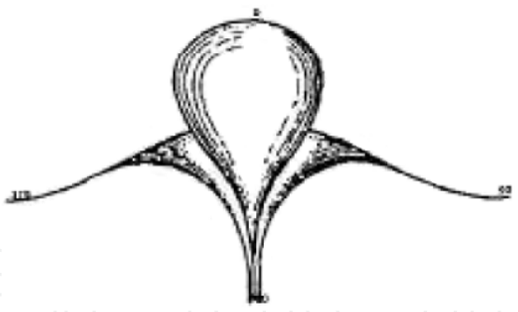

Figure 5. Volcano smoke antennas (1940).

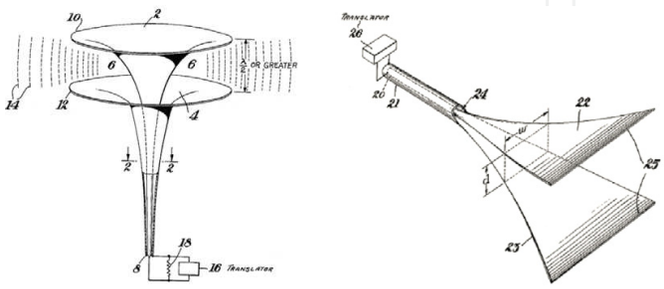

(a) Omni-directional radiation (b) Directional radiation

Figure 6. Brillouin's coaxial horn (1940).

In 1940, J. C. Kraus [5] also developed an antenna similar to the Lindenblad's coaxial horn and named it volcano smoke antenna (See Fig.5), which played a significant role as the cornerstone of television development. Investigations carried out on this antenna showed that this bulbous monopole-like structure yields an impedance bandwidth ratio of 5:1. During that period, coaxial transitions became one of the design techniques for other antenna researchers and designers. In 1948, L. N. Brillouin [6] developed omni-directional and directional coaxial horns, as shown in Fig.6. But these two antennas are difficult to manufacture and use because of their widely structure. Thus, some aspects such as manufacturing cost and complexity of procedures become the important considerations in the design of broadband antennas. The well-known "bow-tie" antenna reveals those benefits, which was originally proposed by Lodge and later rediscovered by G. H. Brown and O. M. Woodward. In 1947, R. W. Masters [7] proposed a similar type of antenna, the inverted triangular dipole, which was later referred to as the "diamond antenna". More recent, other UWB antennas were also developed. W. Stohr [8] introduceed the ellipsoidal monopole and dipole antennas in1968, as shown in Fig. 8. P. J. Gibson proposed the Vivaldi antenna [9] as an amalgamation of slot and Beverage antenna, collectively called tapered slot antenna, in 1979.

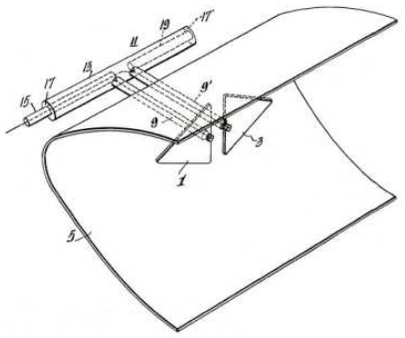

Figure 7. Master's diamond dipole (1947).

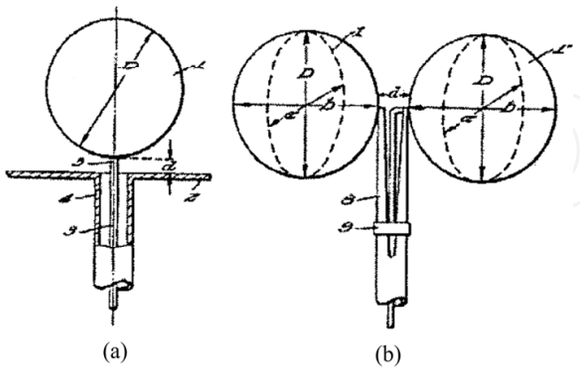

Figure 8. Stohr's ellipsoidal monople and dipole (1968).

The conventional UWB antennas have been wide used in the broadcast communication applications, but they are not suitable for some high frequency applications in modern and further due to their solid structure and un-integration. In the following sections, some new types of UWB antennas will be introduced for high frequency applications..

3. Omni-directional UWB antenna and design

Along with the wireless system miniaturization and operation frequency increasing, some novel types of onmi-directional UWB antennas have been developed in the last decade. Mainly consisting of two types, the UWB planar monopole antenna and the UWB printed monopole antenna, both types are basically developed from the principles of conventional UWB antennas, such as the biconical antenna, the cone-disc antenna, the cage antenna, and etc. Based on several techniques in terms of bandwidth enhancement, omni-directional radiation improvement and size reduction, they can provide almost the same bandwidth and radiation performances as the conventional UWB antennas but with much smaller volumes.

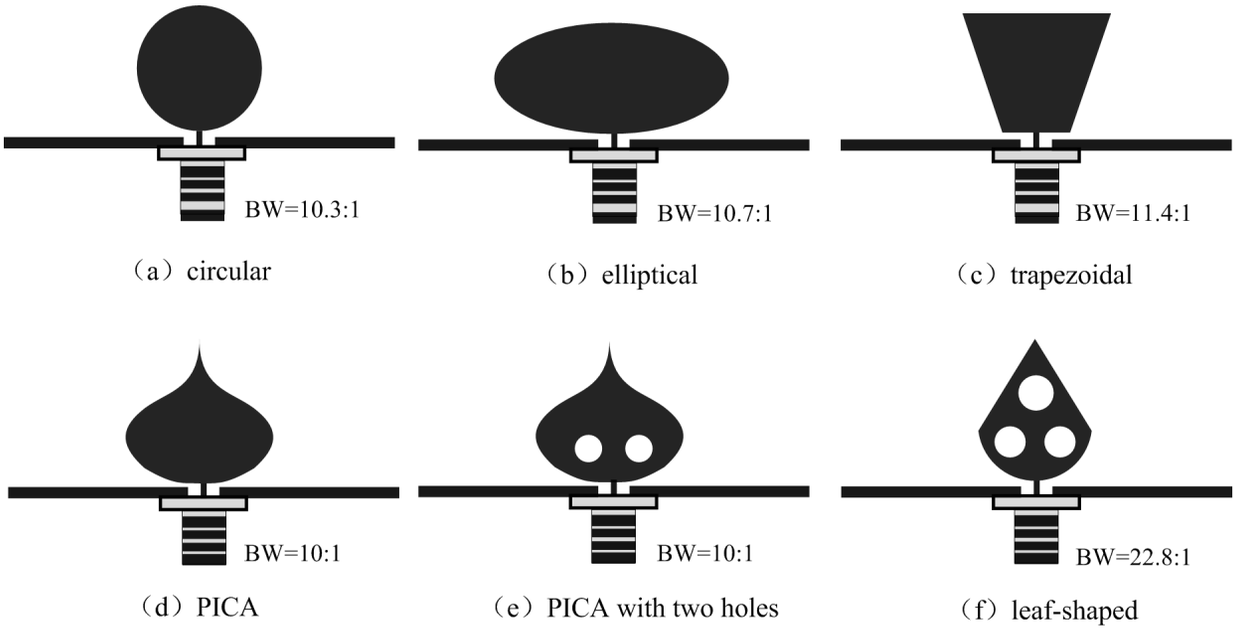

Figure 9. Various geometries of planar monopole antennas [11-14].

3.1. UWB planar monopoles

The planar monopole antenna was firstly reported in 1976 by G. Dubost and S. Zisler [10]. It can be realized by replacing a conventional wire monopole with a planar monopole, where the planar monopole is located above a ground plane and commonly fed using a coaxial probe. Up to now, many planar monopole antennas have been introduced due to their wideband performance. Several representative structures are shown in Fig.9, and these antennas achieve the impedance bandwidth ratio from 2:1 to more than 10:1. *i.e.*, Agrawall *et al.* [11] carried out a bandwidth comparison of several planar monopoles with various geometries, such as circular, elliptical, rectangular, and trapezoidal monopoles. The results show that the circular and elliptical monopoles exhibit much wider bandwidth performance than those of others, and both can obtain the impedance bandwidth ratio

exceeding of 10:1 (Circular monopole: 1.17~12 GHz, Elliptical monopole: 1.21~13 GHz). Evans *et al*. [12] proposed a trapezoidal planar monopole antenna above the ground plane, also achieved a bandwidth ratio exceeding of 11:1. Besides the regular structures, Suh *et al*. [13] proposed an interesting structure, the planar inverted cone antenna (PICA), which can provide an impedance bandwidth ratio of more than 10:1 and the pattern bandwidth ratio of about 4:1. To improve the pattern bandwidth ratio, two circular holes are added in the PICA, as shown in Fig.9(e). This alteration improves the radiation pattern performance dramatically without impairing the impedance performance, where the radiation pattern of the two-circular-hole PICA antenna provides a good omnidirectional performance over a bandwidth ratio up to 7:1 and has a very low cross polarization, 20 dB or less. Later, Bai *et al*. [14] presented a modified PICA, where a leaf-shaped metal plate with three circular holes is vertically mounted on the ground plate and is covered by a dielectric plate instead of the conventional metal plate. It achieves the impedance bandwidth ratio better than 20:1, covering the frequency range from 1.3 to 29.7GHz, as shown in Fig.9(f).

Among various planar monopole antennas, the square planar monopole is the simplest in geometry, and its radiation pattern is usually less degraded within the impedance bandwidth. These favourable features attract many studies, mainly on the bandwidth enhancement since the square planar monopole only owns an impedance bandwidth ratio of 2:1. From the antenna geometry, the feed gap, the feed point location and the shape of the monopole's bottom, all may affect the impedance matching. Thus, several techniques such as notching, bevelling, double feed, trident-shaped feed, and etc., were proposed to expand the bandwidth of the square monopole antenna, as shown in Fig.10 *i.e.*, Su *et al*. [15] proposed a method of cutting a pair of notches at the two lower corners of the square planar monopole. With suitable dimensions of the notches chosen, the impedance bandwidth can be greatly enhanced to be about 3 times that of a corresponding simple square planar monopole antenna (2~12.7 GHz compared to 2~4.5 GHz). Antonino-Daviu *et al*. [16] proposed a method of double feed with aims to intense the vertical current distribution and suppress the horizontal distribution in the square planar monopole, which contributes to improvement in the impedance bandwidth and polarization properties. This method achieves an impedance bandwidth ratio of 9.5:1. However, in this double-feed design, an additional feeding network under the ground plane is required to excite the antenna at two separate feeding positions. To avoid using the external feeding network, Wong *et al*. [17] proposed a trident-shaped feeding strip structure. With the use of a trident-shaped feeding strip, the square planar antenna's impedance bandwidth can be enhanced to be larger than 3.5 times that of a simple feeding strip (1.4~11.4 GHz compared to 1.5 ~3.3 GHz). Moreover, hybrid techniques are also proposed, *i.e.*, Thomas *et al*. [18] used a sleeved transmission line as a transformer together with the bevelling technique, the impedance bandwidth ratio reaches about 12:1 (0.5 ~ 6 GHz). Ammann *et al*. [19] adopted a method of combining the bevelling and the shorting techniques, the square planar monopole antenna's bandwidth ratio can be expanded to more than 13:1 (0.8 ~10.5 GHz).

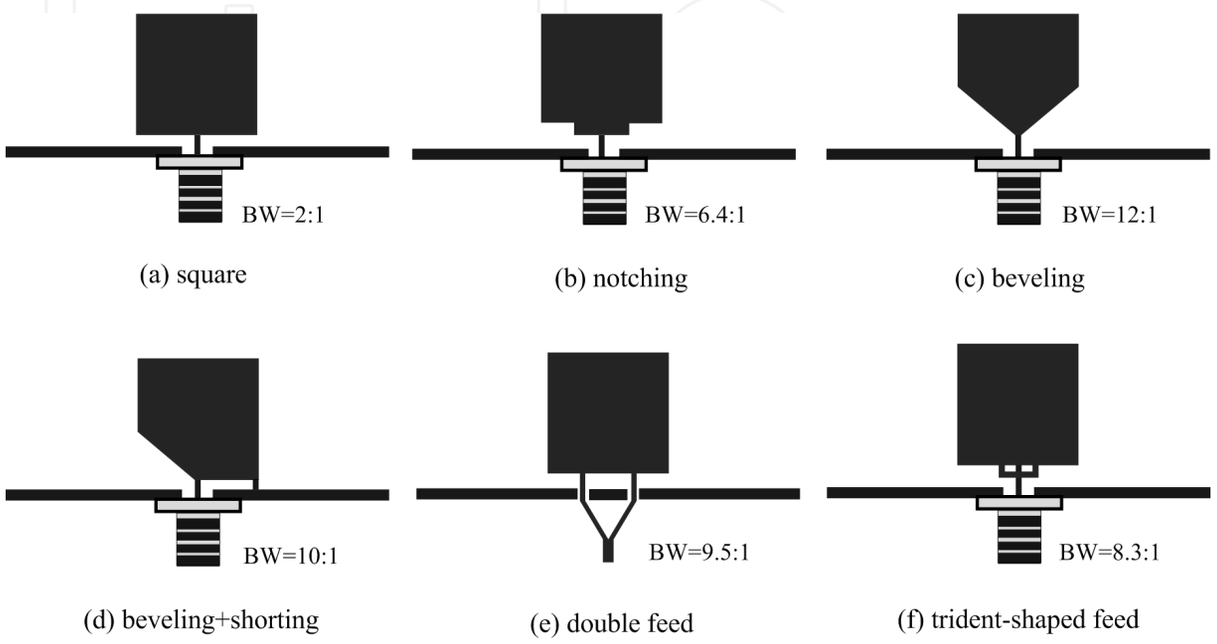

Figure 10. Various wideband techniques for planar square monopole antennas [15-19].

3.2. UWB printed monopoles

The aforementioned planar monopole antennas achieve an ultra-wideband performance based on various techniques, but they all need a perpendicular ground plane, resulting in increasing of the antenna volume and inconvenience for integration with monolithic microwave integrated circuits (MMICs). For the portal wireless device applications, the printed UWB monopole antennas are more popular due to their easier integration than the planar UWB monopole antennas.

The printed UWB monopole antenna commonly consists of a monopole patch and a ground plane. Both of them are printed on the same or opposite side of a substrate, and a microstrip or CPW feedline is used to excite the monopole patch. Since Choi *et al*. [20, 21] introduced this type of antenna with the wideband characteristics in 2004, various printed monopole antennas were studied in the following several years, mainly on the geometries of the monopole and the ground plane.

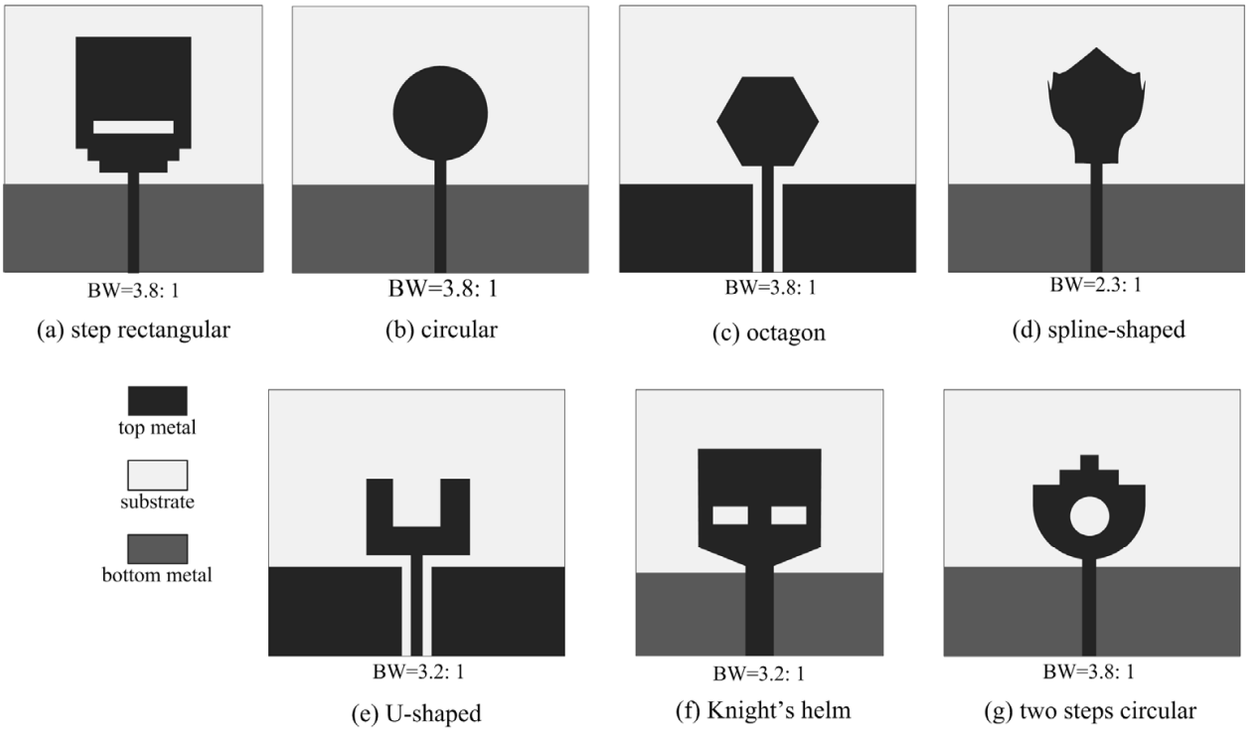

Figure 11. Various monopole structures [21-27].

For geometry of the monopole patch, Fig.11 presents several representative structures. These antennas achieve the impedance bandwidth ratios from 2.3:1 to 3.8:1. Among various geometries of the monopole patches, the printed circular monopole antenna is one of the simplest [22], which achieves the impedance bandwidth ratio of 3.8:1 (2.69~10.16 GHz) with satisfactory omnidirectional radiation properties. Other monopoles such as octagon monopole [23], spline-shaped monopole [24], U-shaped monopole [25], knight's helm shape monopole [26] and two steps circular monopole [27], as shown in Fig.11, were also proposed and studied,. *i.e*., Ooi *et al*. [23] introduced the two-layer octagon monopole antenna based on the low-temperature co-fired ceramic (LTCC) technique, also obtaining an impedance bandwidth ratio of 3.8:1 (3.76~14.42 GHz). Lizzi *et al*. [24] proposed the spline-shaped monopole UWB antenna able to support multiple mobile wireless standards, covering DCS, PCS, UMTS, and ISM bands, with the bandwidth ratio of 2.3:1 (1.7~2.5 GHz).

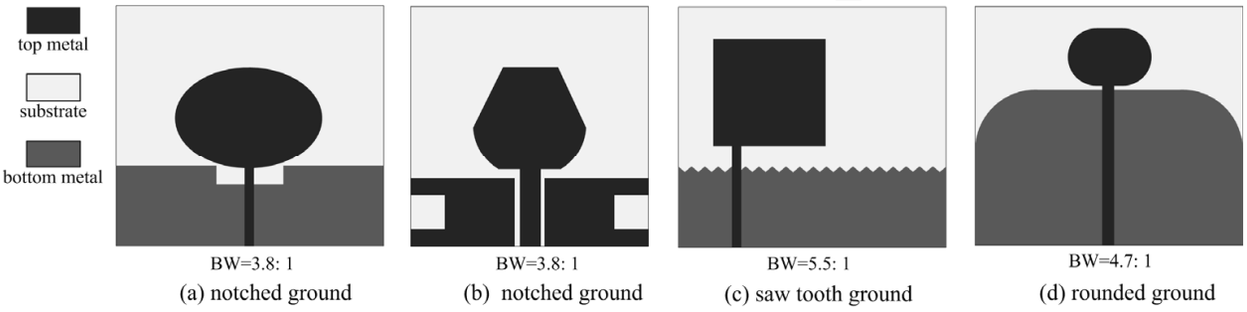

Figure 12. Various ground structures [28-31].

For geometry of the ground plane, several representatives are also shown in Fig.12, and obtain the impedance bandwidth ratios from 3.8:1 to more than 10:1. *i.e.*, Huang *et al*. [28, 29] introduced an impedance matching technique by cutting a notch at the ground plane, and the impedance bandwidth can be enhanced by suitable size and position of notch chosen. Azim *et al*. [30] proposed to improve the impedance bandwidth by cutting triangular shaped slots on the top edge of the ground plane. The printed square monopole antenna with symmetrical saw-tooth ground plane obtains the impedance bandwidth ratio of 5.5:1 (2.9~16GHz). Considering high concentration of currents in the corners of the patch or ground, Melo *et al*. [31] studied a rounded monopole patch with a rounded truncated ground plane. It provides an impedance bandwidth ratio of larger than 4.7:1 (2.55 ~12 GHz).

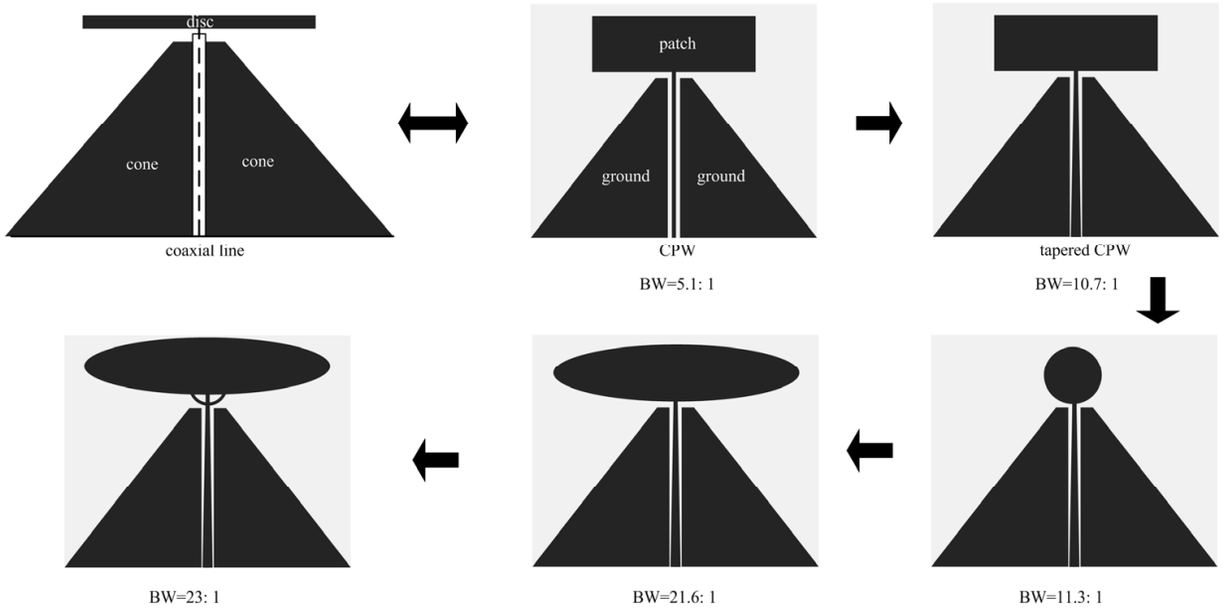

Figure 13. Various printed monopole antennas with trapeziform ground [32-36].

One of interesting UWB printed monopole antenna designs is a trapeziform ground plane with a rectangular patch monopole aroused from the discone antenna, where the rectangular patch is used to replace the disc, the trapeziform ground plane is used to replace the cone, and the CPW is used to replace the coaxial feed, as shown in Fig.13 [32]. It is found that the printed rectangular antenna with a trapeziform ground plane achieves an impedance bandwidth ratio of 5.1:1, which is similar to that of a discone antenna. To enhance the bandwidth further, the input impedance is investigated by comparing bandwidths for various characteristics impedance of CPW feedline. The impedance bandwidth ratio expands to 12:1 when the characteristic impedance of CPW feedline is about 100Ω, which means the impedance bandwidth is enhanced by a factor of about 2.3. In order to match 50Ω SMA or N-type connectors, a linearly tapered central strip line is used as an impedance transformer, and an impedance bandwidth ratio of 10.7:1 (0.76~11 GHz) is obtained. Moreover, various printed monopoles and feed structures are also studied to enhance the bandwidth further [33-36].

In fact, geometries of the monopole and the ground plane not only affect the antenna impedance bandwidth but the antenna radiation pattern and phase center over a wide bandwidth, which is an important phenomenon, especially for pulsed devices that need minimum signal distortion. Thus, the relation between antenna structure and its radiation are also studied. *i.e.*, Fortino *et al*. [37] introduced a CPW-fed printed triangular monopole antenna with a specific ground plane, such as the double folded structure, where the ground plane is optimized to obtain more constant radiation patterns versus frequency. Wu *et al*. [38] also pointed out the ground plane may affect the antenna's H-plane radiation pattern as its width could be comparable with the wavelength at the higher operating frequency. Thus, a compact ground plane with a trident-shaped feed structure is proposed to significantly improve the H-plane radiation pattern in a very wide impedance bandwidth, as shown in Fig.14.

Moreover, the wireless portable devices become smaller and smaller, which contributes the printed UWB antenna design on miniaturization. One of creative miniaturization techniques is proposed by Sun *et al*. [39], where a 40% size reduction is realized by simply exploiting its structural symmetry, as shown in Fig.15. It is found that the miniaturized bevelled planar monopole antenna exhibits a much wider impedance bandwidth, higher cross-polar radiation, and slightly lower gain at higher frequencies as compared with its un-miniaturized counterpart.

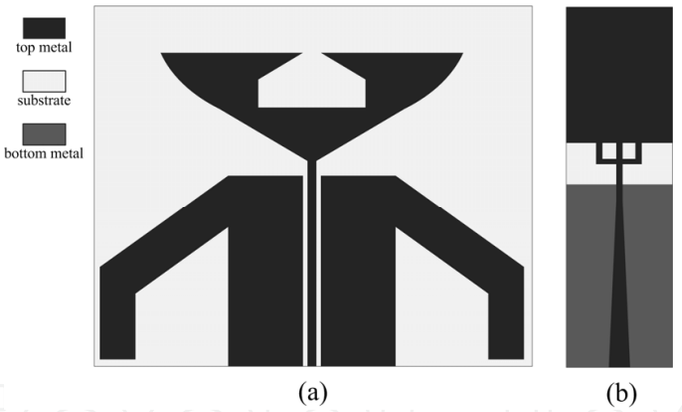

Figure 14. Radiation improvement techniques [37, 38].

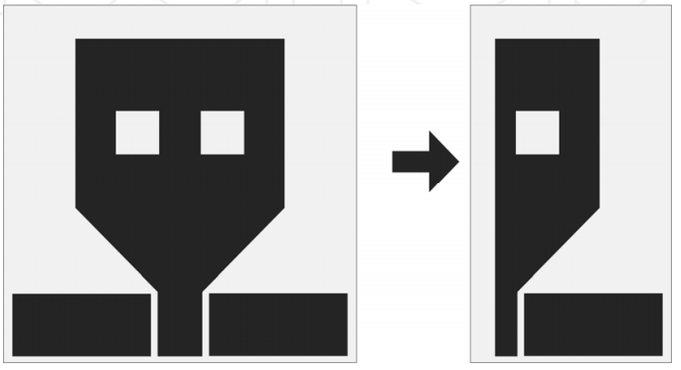

Figure 15. Miniaturization techniques [39].

4. Directional UWB antenna and design

Comparing to the omni-directional UWB antenna, the directional UWB antenna with a much higher gain is also required to meet various applications. In this section, several types of directional UWB antenna design such as the UWB printed wide-slot antennas, the UWB DRAs, and the DRAs with radiation reconfiguration, etc., are detail introduced.

4.1. UWB printed wide-slot antenna

The printed wide-slot antenna is another type of the most suitable candidates for UWB applications. This type of antenna is commonly consists of a wide-slot and a tuning stub connected with a microstrip or CPW feedline. Up to now, many wide-slot antennas, including different wide-slots or tuning stubs, have been extensively studied on the antenna operation bandwidth. Among various shapes of slot, the rectangular wide-slot is the simplest structure. Based on the rectangular wide-slot, several shapes of the tuning stub are studied, where the representative geometries are shown in Fig.16 and the bandwidth ratios vary from 1.8:1 to 3.6:1. *i.e.*, Jang *et al*. [40, 41] presented two rectangular wide-slot antennas fed by the microstrip line with a cross-shaped stub and a Π-shaped stub, respectively. The antenna bandwidth greatly depends on the length of the horizontal and vertical feed lines as well as on the offset position of the feedline. The two slot antennas achieve the impedance bandwidth ratios of 2.8:1 (1.7~ 4.9 GHz) and 3.5:1 (1.7~ 6.0 GHz), respectively. Later, Yao *et al*. [42] proposed a fan-shaped microstrip stub together with a strip, which contributes to a little wider with the bandwidth ratio of 3.6:1 (0.5~ 5.7 GHz). A rectangular slot with a rectangular tuning stub was also studied [43], but with the bandwidth ratio of 1.8:1.

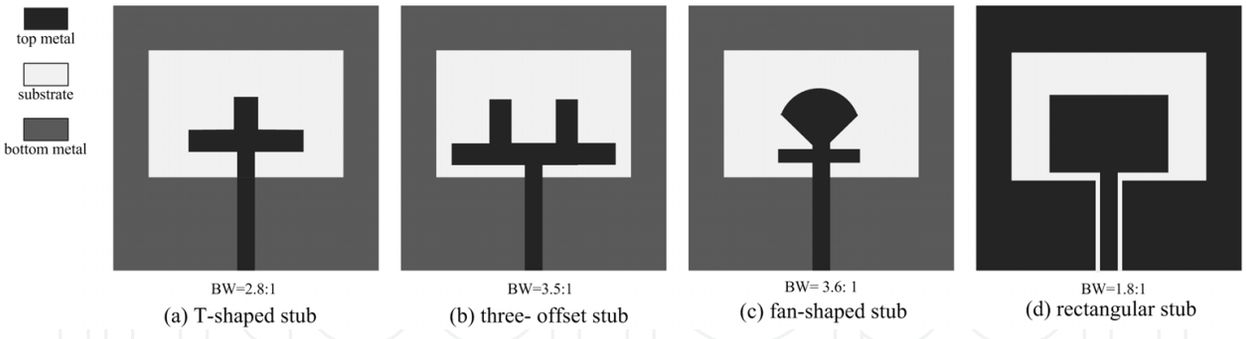

Figure 16. Various shapes of tuning stubs [40-43].

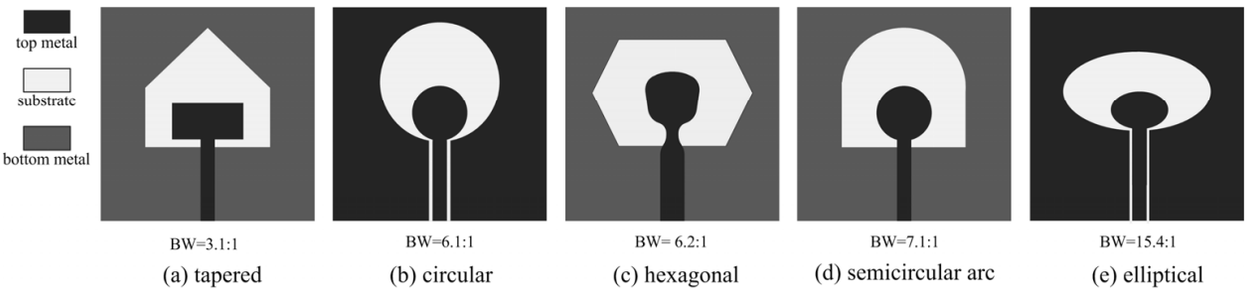

Figure 17. Various shapes of wide-slots [44-48].

It is also noted that the slot shape plays more important on affecting the antenna bandwidth compared to the tuning stub shape. Fig.17 gives several shapes of wide-slots, such as the tapered slot, the circular slot, the hexagonal slot, and etc. These antenna can provide the impedance than ratios from 3.1:1 to 15.4:1, which are much wider bandwidth those of rectangular wide-slot antennas. *i.e.*, Azim *et al*. [44] presented a tapered-shape slot excited by a rectangular tuning stub, which achieves an impedance bandwidth ratio of 3.1:1 (3~11.2 GHz) with a stable gain and radiation over the bandwidth. Denidni *et al*. [45] proposed a circular slot fed by a circular patch through a CPW feedline. This configuration offers a much larger bandwidth ratio of 6.1:1 (2.3~13.9 GHz). Furthermore, Angelopoulos *et al*. [46] investigated the elliptical slot with an elliptical tuning stub achieving an impedance bandwidth ratio of 15.4:1 (1.3~20 GHz), which is the widest bandwidth of the printed slot antennas in open literature.

Different from above regular shapes of the slot or tuning stub, several special geometries of printed slot antennas, such as dual annular slot, semi-elliptic slot, and etc., were also introduced for UWB applications, as shown in Fig.18. These antennas achieve the impedance bandwidth ratios from 3.7:1 to 7:1. For instance, Ma *et al*. [49] introduced a tapered-slot-fed annular slot antenna. The tapered-slot feeding structure serves as an impedance transformer and guides the wave propagating from the slot line to the radiating slot without causing pernicious reflection. The radiating slot is curved to distribute part of the energy to the reverse side of the feeding aperture. This antenna achieves an impedance bandwidth ratio of 3.7:1 (2.95~11 GHz). Gopikrishna *et al*. [50] introduced a semi-elliptic slot antenna. The antenna features a CPW signal strip terminated with a semi-elliptic stub and a modified ground plane to achieve a wide bandwidth ratio of 7:1 (2.85~20 GHz). Pourahmadazar *et al*. [51] studied a special square slot antenna for circular polarization, which is composed of a square ground plane embedded with two unequal-size inverted-L strips around two opposite corners of the square slot. The antenna owns an impedance bandwidth ratio of 4.7:1 (2.67~13 GHz) and a circular polarization bandwidth ratio of 1.5:1 (4.9~6.9 GHz). Sim *et al*. [52] proposed a compact microstrip-fed narrow slot antenna design for UWB applications. By properly loading a notch to the open-ended T-shaped slot and extending a small section to the microstrip feedline, an impedance bandwidth ratio of 3.7:1 (3.1 ~11.45 GHz) is obtained.

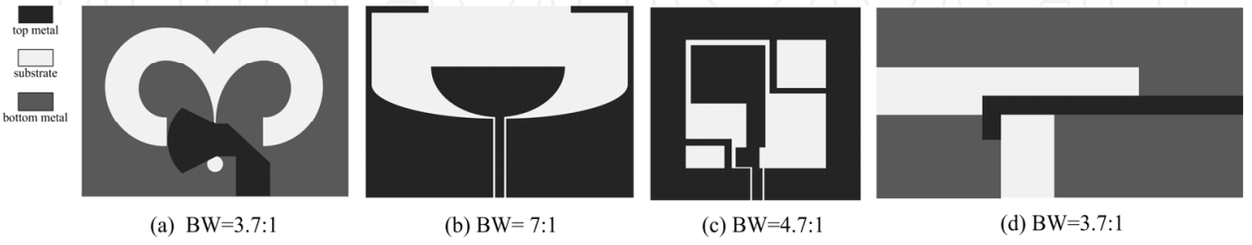

Figure 18. Special geometries of wide-slot antennas [49-52].

Commonly, the operation bandwidth depends on the requirement of the wireless communication system which needs various bandwidths. From above mentioned slot antennas, it is known that the printed wide-slot antenna may achieve a wide range

bandwidth based on design of various special slots or stubs. Unfortunately, it maybe wastes a lot of time for antenna designers to find a suitable slot antenna structure according to a required operation bandwidth. So the investigation on the relationship between the slot structure and the bandwidth becomes very useful. For this purpose, reference [53] presented an interesting deep study on printed binomial-curved slot antennas, where the slot and the tuning stub both formed by a binomial curve function, thus various bandwidths can be obtained based on the structure with different binomial curves.

The CPW-fed printed binomial-curved slot antenna is shown in Fig.19. It consists of a wide slot, a tuning stub, and a CPW feedline, all printed on a single-layer metallic substrate of thickness h and relative permittivity ε_r, and with dimension of $L \times W$. The slot's outline size is denoted as $l \times w$, where the coordinate of point **A** on the up-right of the slot is fixed to (w/2, l) and the edge is formed by a binomial curve function, expressed as follows:

$$y = f_1(x) = l \cdot (2x / w)^N, \qquad 0 \le x \le w/2 \tag{3}$$

where N is the order of the binomial curve function. The slot is excited by a CPW feedline, where the signal strip width is w_f, and the gap spacing between the signal strip and the coplanar ground plane is g. To achieve an efficient excitation and a wide impedance matching, the signal strip is terminated to a tuning stub with the same shape as the slot but with a smaller size, which has an offset d away from the bottom edge of slot. The stub-to-slot's outline size-ratio is denoted as τ. Therefore, the coordinate of point **B** on the upper-right of the tuning stub is denoted as (τw/2, τl+d), and the binomial curve function for the edge of the tuning stub can be rewritten as follows:

$$y = f_2(x) = d + \tau l \cdot (2x / \tau w)^N, \qquad 0 \le x \le \tau w/2 \tag{4}$$

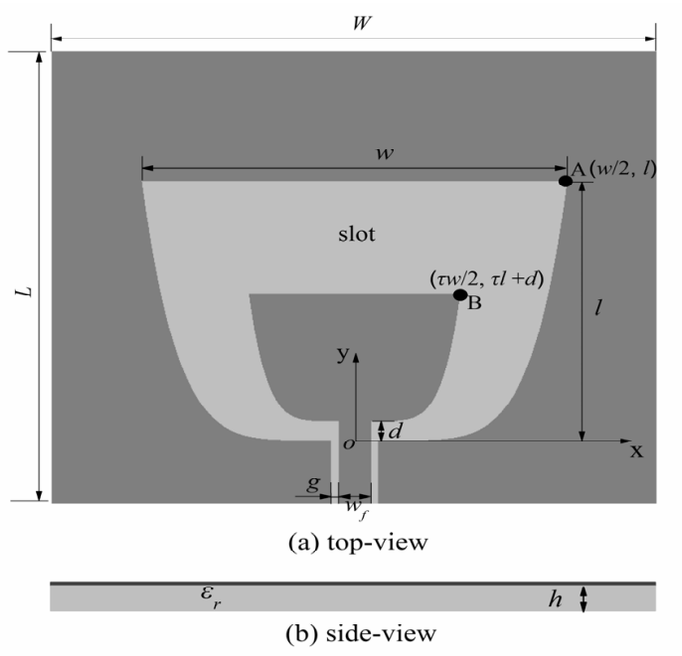

Figure 19. Binomial slot antennas.

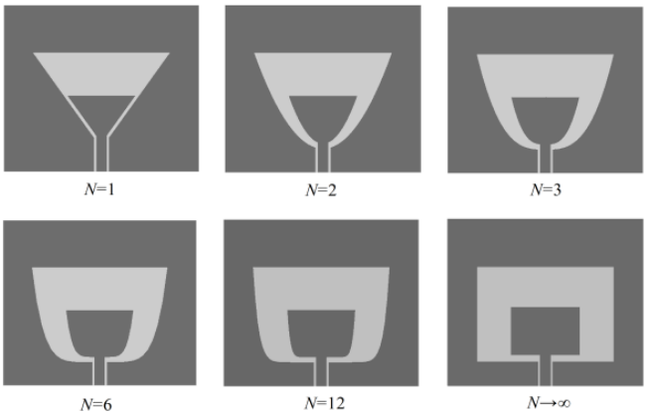

Figure 20. Various binomial slot antennas.

Several shapes for different N are given in Fig.20. As N equals to 1, both the slot and the tuning stub are the triangular shape. As N increases, the bottom widths of the slot and the tuning stub expand gradually, and their shapes look like bowls. As N approaches infinity, both the slot and the tuning stub are transformed to the rectangular shape. From Fig.21, it is found that the operation bandwidth range varies from 10~20 % to 20~40 %, 25~60 %, 60~90 %, 70~110% and 85~110%, as the order N increases from 1 to 2, 3, 6, 12 and ∞, respectively, meaning that the larger order N is selected, the wider bandwidth may be obtained. It is also known that a proffered wideband slot antenna can be easily designed based on suitable selection of parameters, such as w/l, N, according to the operation bandwidth in applications, which is convenient for the wideband antenna design.

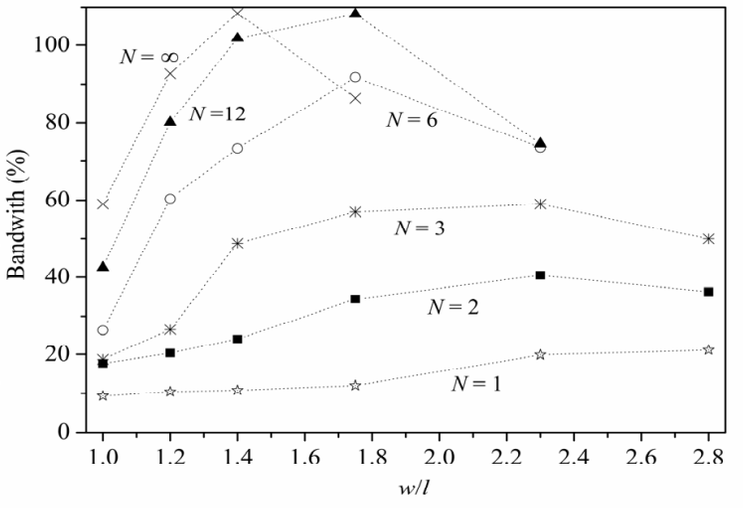

Figure 21. Various bandwidths for orders N.

4.2. UWB dielectric resonator antenna

Dielectric resonator antenna is a new type of directional UWB antenna. It owns a much smaller size and higher efficiency than the UWB printed monopole and wide-slot antennas. Recently, many studies have been proposed to expand the DRA's bandwidth and promote it

into the UWB antenna. One of effective methods to expand the DRA's bandwidth is the hybrid technique, which combine the DRA and the monopole antenna. Both antennas provide the similar radiation patterns but with different operation frequency bands. Several representative UWB hybrid DRAs are shown in Fig.22 *i.e.*, Lapierre *et al*. [54] firstly proposed a hybrid antenna design by combining the properties of a quarter wavelength monopole antenna with an annular DRA. This design can be used to retrofit existing monopole antennas: by introducing an appropriate DRA, the original narrow-band monopole can be transformed to achieve an UWB performance, with bandwidth ratio of 2.6:1 (6.5~16.8 GHz). To enhance the antenna bandwidth further, Ruan *et al*. [55] proposed a double annular ring DR with different permittivity, which achieves an impedance bandwidth ratio of 3.7:1 (1.8~6.9 GHz). Later, Jazi *et al*. [56] proposed a skirt monopole antenna used to excite an inverted conical-ring-shape dielectric resonator. In this design, three different methods of impedance matching, dielectric, and ground plane shaping procedures have been applied to increase the antenna bandwidth. The results show that by shaping the dielectric structure and impedance matching method, the input impedance and location of the higher part of the frequency bandwidth can be controlled by exciting higher order mode ($TM_{012+\delta}$) of the same family with dominant resonant mode inside the DR ($TM_{01\delta}$). The lower part of the input impedance bandwidth can be adjusted using the ground plane shaping and matching method at the feed. This antenna achieves the bandwidth ratio of 3.8:1 (1.8~6.9 GHz).

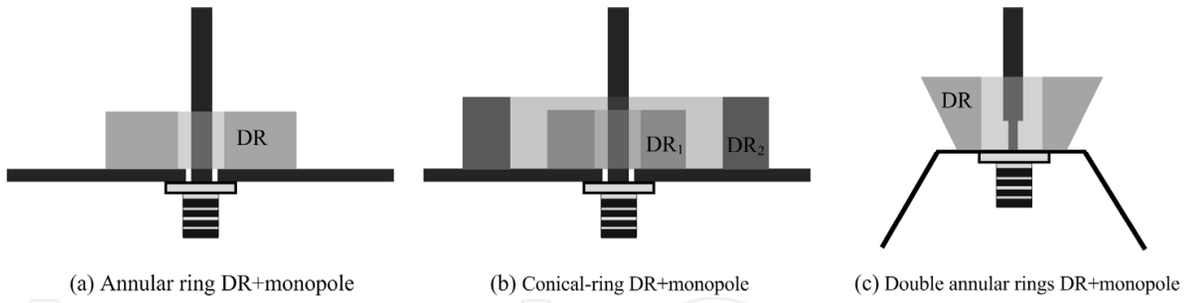

Figure 22. UWB hybrid DRAs [54-56].

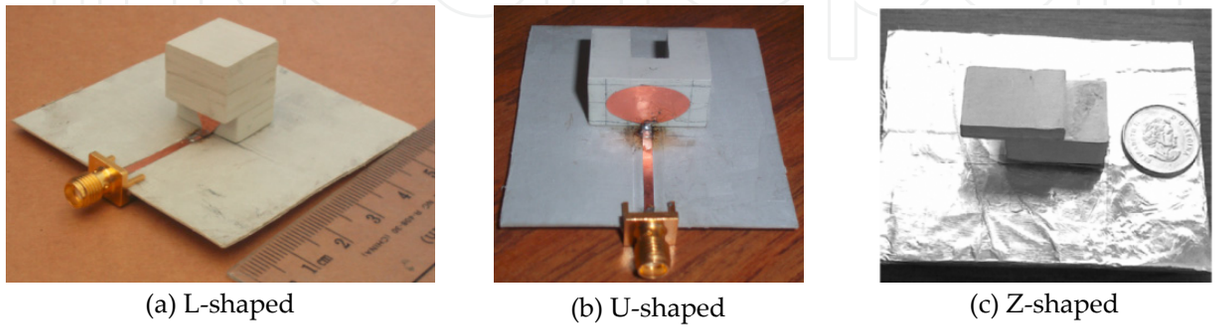

Figure 23. Photos of various UWB DRAs [58-60].

Apart from the UWB hybrid DRA design, recently, Liang *et al*. [57-61] proposed a patch feed technique and DRAs with various alphabet structures, such as cross-T-shaped [58], L-shaped [57], U-shaped [59], and Z-shaped [60], as shown in Fig.23, where the DRA bandwidth ratios of 2.1:1~9.4:1 were obtained. Fig.24 presents the trapezoidal patch-fed L-shaped DRA design process. To explain the wideband operation of the patch-fed L-shaped DRA, three reference antennas are used as references. Fig.24 (a) is a rectangular DR on a ground plane; Fig.24 (b) is a rectangular DR on a single-sided copper-clad substrate, and Fig.24 (c) is an L-shaped DR on a single-sided copper-clad substrate. The three antennas are excited by the probe feed mechanism and their optimized numerical results in terms of bandwidth are compared with patch-fed L-shaped DRA, as shown in Fig.24. It is observed that the impedance bandwidth can be expanded by using an inserted intermediate substrate, an L-shaped DR, and an inverted-trapezoidal patch feed mechanism. Table 1 lists several proposed UWB DRAs, including the antenna geometry, the feed mechanism and the bandwidth.

The above mentioned UWB antennas could provide the monopole-like radiation or mushroom-like radiation in an ultra-wideband. While some portal UWB wireless devices need both the monopole-like radiation and the mushroom-like radiation since their position are not fixed in communication. For this purpose, Liang *et al*. [62] proposed a UWB DRA with the configurable radiation pattern design, where a rectangular DR excited by dual bevel-rectangular patches. Two bevel-rectangular metal patches are attached on the opposite sides of the DR for excitation and both connect to the 50-ohm microstrip lines, as shown in Fig.25. The bevel-rectangular patch-fed DRA has been proposed to achieve an UWB operation. A reconfigurable radiation pattern performance in terms of the monopole-like radiation and the mushroom-like radiation is obtained through the in-phase feed and the out-phase feed of two input ports, respectively. For the in-phase feed, the antenna performs the monopole-like radiation pattern in the entire operation band. While for the out-phase feed, the antenna performs the mushroom-like radiation in the same operation band.

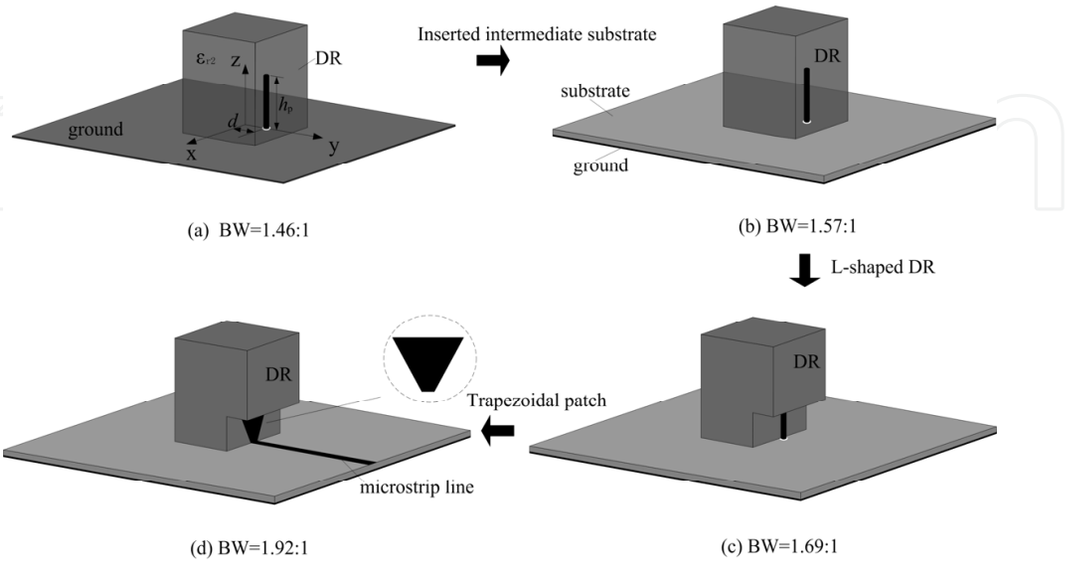

Figure 24. Wideband DRA design.

No	Antenna Geometries	Feed mechanisms	ε_{DR}	VSWR ≤ 2	
				Frequency range	Bandwidth ratio
1	Annular ring DR+monopole [54]	probe	10	6.5~16.8 GHz	2.6:1
2	Double annular-ring DR+monopole [55]	probe	4&36	3~11.2 GHz	3.7:1
3	Conical-ring DR + skirt monopole [56]	probe	10	1.8~6.9 GHz	3.8:1
4	L-shaped DR [57]	Trapezoidal patch	9.8	3.87~8.17 GHz	2.1:1
5	Cross-T-shaped DR [58]	Trapezoidal patch	9.8	3.56~7.57 GHz	2.1:1
6	U-shaped DR [59]	Triangle patch	9.8	3.1~7.6 GHz	2.4:1
7	Z-shaped DR [60]	Beveled rectangular patch	9.8	2.5~10.3 GHz	4.1:1
8	Circular DR [61]	Crescent patch	35	1.6~15 GHz	9.4:1
9	Rectangular DR[62]	Bevel-rectangular patch	9.8	3.9~12.2 GHz	3.1:1

Table 1. Various bandwidths of UWB DRAs.

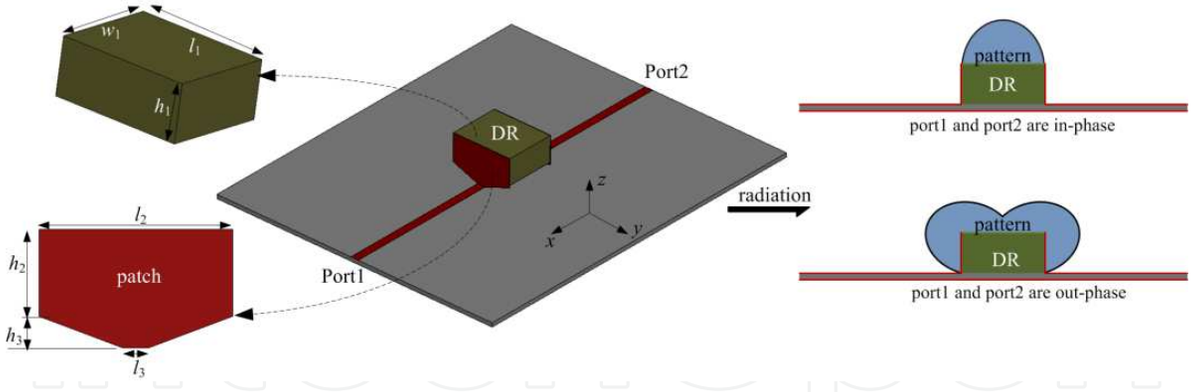

Figure 25. UWB DRAs with a radiation reconfiguration.

5. Band-notched UWB antenna and design

The Federal Communication Commission released the frequency band 3.1~10.6 GHz for the UWB system in 2002. But along with the UWB operating bandwidth, there exist some narrowband wireless services, which occupy some of the frequency bands in the UWB band. The most well-known among them is wireless local area network (WLAN) IEEE802.11a and HIPERLAN/2 WLAN operating in 5.15~5.35 GHz and 5.725~5.825 GHz bands. Apart from WLAN, in some European and Asian countries, world interoperability for microwave access

(WiMAX) service from 3.3 to 3.6 GHz also shares spectrum with the UWB. This may cause interference between the UWB system and other exist communication systems. To address this problem, one way is to use filters to notch out the interfering bands. However, the use of an additional filter will result in increasing the complexity of the UWB system and also the insertion loss, weight and size for the UWB trans-receivers. Therefore, various UWB antennas with notched functions have been researched to overcome this electromagnetic interference. This section concludes the existing band-notched techniques, which can be classified into the following categories: embedding slot, parasitic stub, bandstop transmission line, and hybrid techniques.

5.1. Embedding slot

Among various proposed techniques on the band-notched UWB antenna design. One common and simple way is to etch slots on the radiation patch or ground plane. Up to now, many shapes of embedding slots were studied, and some representatives are shown in Fig.26 *i.e.*, Kim *et al*. [63] proposed a CPW-fed planar UWB antenna with a hexagonal radiating element. By inserting a V-shaped thin slot with a length of $\lambda c/4$ (λc is the wavelength of notched frequency) on the hexagonal radiating element, the narrow frequency band-notched is created, where the fractional bandwidth is approximately 8~10%. Chung *et al*. [64-66] introduced the printed UWB monopole antenna by inserting an inverted U-shaped, Π-shaped or rectangular slot. At the notched frequency, current is concentrated around the edges of the slot and is oppositely directed between the interior and the notched frequency. This leads to the desired high attenuation near the notched frequency. In [67], a band-notched printed monopole antenna is provided by using two modified U-shaped slots on the monopole. The U-shaped slot perturbs the resonant response and also acts as a half-wave resonant structure. At the notched frequency, the desired high attenuation near the notched frequency can be produced. Jiang *et al*. [68, 69] introduced a pair of inverted-L-shaped slots around the microstrip line on the ground plane; a frequency-notched response can also be achieved.

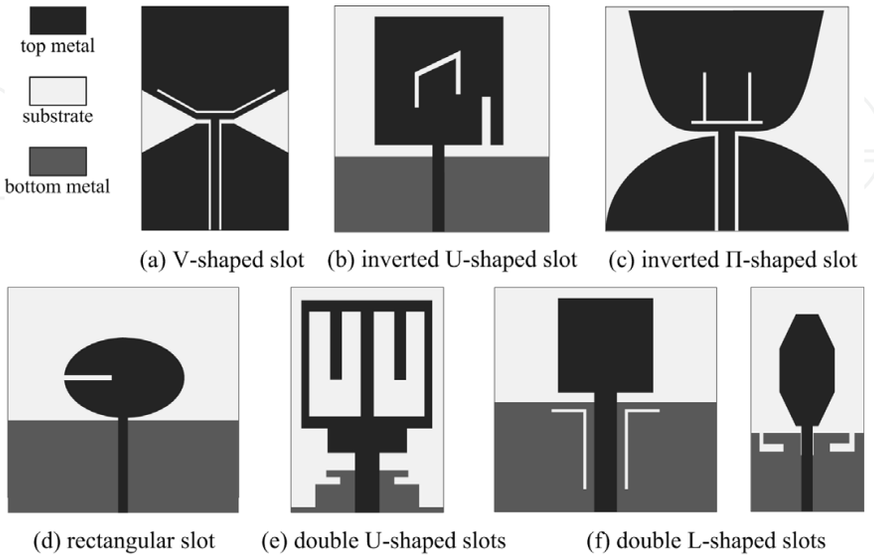

Figure 26. Notched-band designs with various slots on patch or ground [63-69].

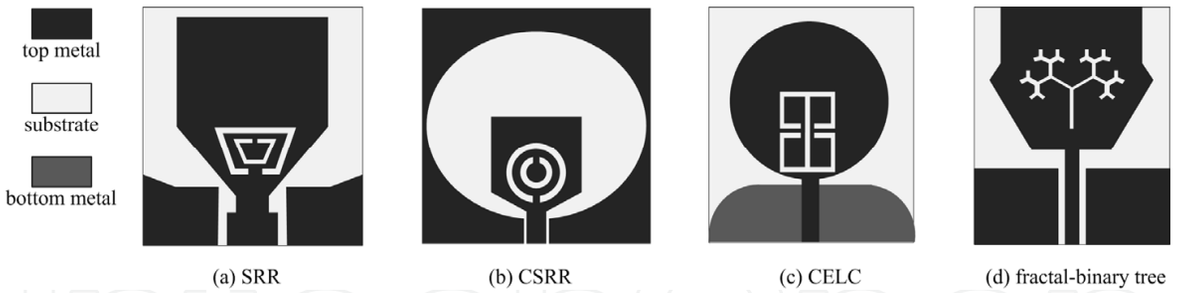

Figure 27. Notched-band designs with various periodic structure slots [70-73].

Since split-ring resonator (SRR), electric-LC (ELC) resonator, complementary split-ring resonator (CSRR) and complementary electric-LC (CELC) resonator are commonly used to design a material with negative permittivity and permeability, all these structures can also be applied in UWB antennas for the notched band design. Several representatives are shown in Fig.27. The SRR is generally composed of two concentric split ring strips. It has a favourable aspect in size since it can be designed as small as one-tenth of the resonance wavelength. In [70], a dual reverse split trapezoid slots, instead of the conventional strip-type SRRs, was proposed and implemented for a bandstop application. In [71], a slot-type CSRR is etched inside the tuning stub of the printed elliptical slot antenna, and implemented for a band-stop application. It was found that an alterable notched band could take place by adjusting the radiuses of the CSRR. In [72], the CELC resonator is etched inside the circular patch of the monopole antenna to achieve the notched frequency band. The CELC could provide a predominantly magnetic response. At the notched frequency, the current flows into the CELC region so that the desired high attenuation near the notched frequency would be produced. In [73], a fractal-binary tree slot embedding technique for the band-notched characteristics design was introduced. By etching a dual band-notched resonance slot using a four-iteration fractal binary tree, two additional filters are applied to the radiating element of the antenna. The fractal, which effect increases the possible length of isolated current paths on the radiating element, has clear and useful properties for band-stop design within small antenna footprints.

5.2. Parasitic stub

Similar to the embedding slot technique in the UWB antenna design, another commonly used technique is a parasitic strip or stub in the aperture area of the antenna or a nearby radiator that forms a resonant structure and leads to a sudden change in the impedance in the notched band. Many parasitic strips or stubs were studied and several representative structures are presented in Fig.28.

For the UWB printed wide-slot antenna design, Liu *et al*. [74] proposed a UWB rectangular slot antenna with a fractal tuning stub to realize the notched function. Chui *et al*. [75] proposed a branch with a length of a quarter of the wavelength adding on the tuning stub to obtain the band-notched property. Cai *et al*. [76] studied a pair of elliptic arc-shaped strips inserted into a suitable aperture region to disturb the field distribution that generates the resonance at the designed notched-band. The total length of this pair of strips is adjusted to about half-wavelength at the desired notched-band, resonance will occur at the strips.

For the printed UWB monopole design, Zhang *et al*. [77] introduced a segmented circular planar monopole antenna with a notched band. Through cutting apart a circular monopole patch with a pair of symmetrical slots, the patch is divided into three segments: the center patch and two side patches. Practically, the side patches function as two parasitic elements and work as bandstop filters. Then, the band-notched property is achieved. Wu *et al*. [78] introduced a square looped resonator and an end-coupled resonator to achieve the gain suppression in the notched band. The square-looped resonator consists of two square loops whose physical length approximates half a wavelength at the notched frequency. Meanwhile, the end-coupled resonator is composed of a strip line with a pair of quarter wavelength folded open stubs. Compared with the band-notched methods using thin slits and plastic strips, this resonator has a small size and a fast rolloff rate well as 10 – 25 dB gain suppression (generally, the gain suppression of thin slits and plastic strips are usually less than 10 dB).

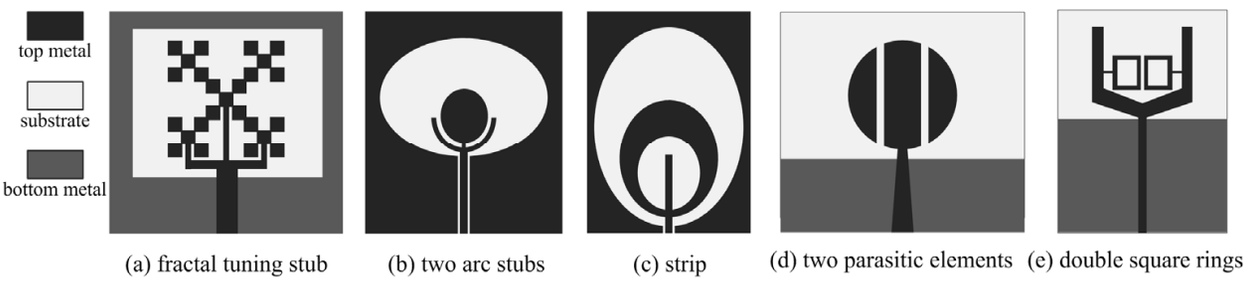

Figure 28. Notched-band designs with various stubs [74-78].

5.3. Bandstop transmission line

The above mentioned notched-band techniques, such as embedding slot or ELC resonator, parasitic stub, will result in affecting the antenna radiation, especially for increasing of the cross-polarization. A transmission line with a bandstop characteristic to feed the UWB antenna can be considered as an integration design of the printed UWB antenna and the filter, which may have little affection to the antenna radiation. Several designs of microstrip feedline with the notched-band function are proposed, as shown in Fig.29 *i.e.*, Zhang *et al*. [79] proposed a U-shaped slot embedded in a microstrip feedline, and a band-notched characteristic was realized. Later, Nouri *et al*. [80] used the defect ground technique to realize the microstrip filter, where a vertical metal strip connected to the rectangular ring is embedded in the shovel-shaped slot that is located under the feedline at the center of ground plane. The notched frequency can be controlled by adjusting the dimensions of the filter structure. Moreover, the electromagnetic band-gap (EBG) structure has a characteristic of preventing wave propagation in special directions or at certain frequencies. In [81], square EBG cells are placed close to the microstrip feedline to obtain the desired notched bands. In [82], the dual band-notched characteristic has been achieved by introducing two open-circuited stubs from two sides of the microstrip feedline. By adjusting the length of two open circuited stubs approximately to one quarter of wavelength, a destructive interference of the current distribution takes place causing the antenna non-radiating at that notched frequency.

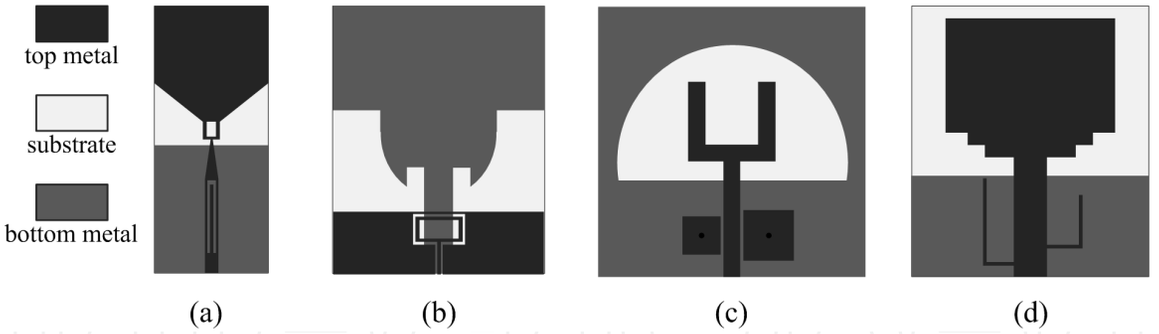

Figure 29. Various bandstop transmission lines [79-82].

5.4. Hybrid techniques

Using one notched-band technique will face two problems. Firstly, it is relatively difficult to create multiple frequency notches with a sharp and narrow stop band. Secondly, multi-notched bands do not have any means to control independently because of the same technique. Therefore, various notched-band techniques have been together used to realize the WiMAX and WLAN bands rejection. The representative hybrid techniques are shown in Fig.30 *i.e.*, Abdollahavand *et al*. [83] studied the hybrid technique by adding parasitic strip and bandstop transmission line. A compound band-notched structure is formed by embedding Γ-shaped stubs in the radiation patch and a modified G-slot defected ground structure in the feeding line, which can provide two filtering frequencies in a certain band and function as a second-order filter. Ye *et al*. [84] studied the hybrid technique of a parasitic strip and a parasitic slit, where the parasitic strip is embedded inside the polygon slot and an isolated slit employed in the beveled T-stub. The desired excellent band-notched UWB operation can be obtained by choosing the sizes of the parasitic strip and slit. Zhou *et al*. [85] presented the hybrid technique of adding parasitic and embedding slot to realize dual notched bands of WiMAX and WLAN. Firstly, the circular patch is cut to an annular ring and a pair of Y-shaped strips is connected to the annular ring, the notched band of WiMAX centered at 3.5 GHz is realized. Then, an inverted V-shaped slot is etched on the patch, a notched band of 5.2 – 5.98 GHz for WLAN band is achieved. Niu *et al*. [86] used the hybrid technique of CCRC resonator and embedding slot, where a CCRC is to realize the 5 GHz WLAN notched-band and an elliptic arc-shaped slot is to realize the WiMAX notched band. Kim *et al*. [87] suggested a triple-band notched hybrid technique, which is based on a geometric combination of a meander shaped stub and the two rectangular complementary split ring resonators (CSRRs) on the feedline, and an inverted U-shaped slot on the center of the patch.

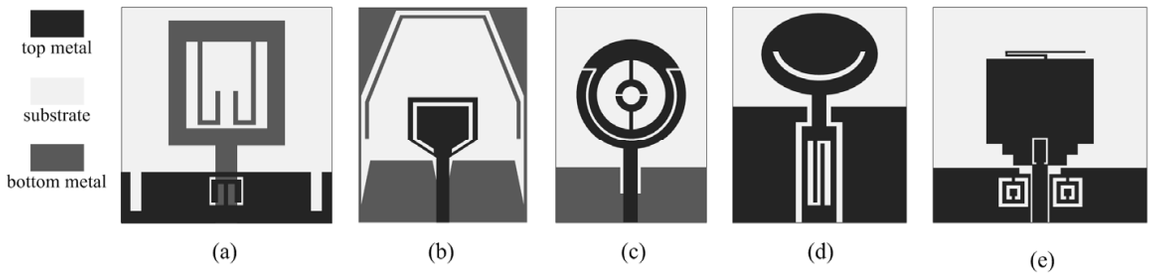

Figure 30. Hybrid notched-band techniques [83-87].

Author details

Xian Ling Liang
Department of Electronic Engineering, University of Shanghai Jiao Tong, P.R. China

6. References

[1] Lodge, Electric telegraphy. U.S. Patent 609,154 (August 16, 1898).
[2] Carter PS. Wideband, short wave antenna and transmission line system. U.S. Patent 2,181, 870 (December 5, 1939).
[3] Schelkunoff SA. Advanced antenna theory. New York: John Wiley and Sons; 1952. p 160.
[4] Lindenblad NE. Wide Band Antenna. U.S. Patent 2,239,724 (April 29, 1941).
[5] Paulsen L, West JB, Perger WF, Kraus J. Recent investigations on the volcano smoke antenna. IEEE Antennas and Propagation International Symposium (Digest), Columbus, OH, Jun. 2003.
[6] Brillouin LN. Broad Band Antenna. U.S. Patent 2,454,766 (November 30, 1948).
[7] Masters RW. Antenna, U.S. Patent 2430353 (November 4, 1947).
[8] Stohr W. Broadband ellipsoidal dipole antenna. U.S. Patent 3,364,491, (January 16, 1968).
[9] Gibson PJ. The Vivaldi aerial, Proc. 9th Europe Microwave Conf., Brighton, U.K. 1979.
[10] Dubost G and Zisler S. Antennas a Large Bande. New York: Masson, 1976.
[11] Agrawall NP, Kumar G, and Ray KP. Wide-band Planar Monopole Antennas. Transactions on Antennas and Propagation 1998 ; 46(2): 294-295.
[12] Evans JA and Ammann MJ. Planar Trapezoidal and pentagonal monopoles with impedance bandwidth in excess of 10:1. IEEE Antennas and Propagation International Symposium (Digest), Orlando, FL; 1999.
[13] Suh SY, Stutaman WL and Davis WA. A new ultrawideband printed monopole antenna: the Planar Inverted Cone Antenna (PICA). IEEE Transactions on Antennas and Propagation 2004; 52(5): 1361-1365.
[14] Bai XF, Zhong SS and Liang XL. Leaf-shaped monopole antenna with extremely wide bandwidth. Microwave and Optical Technology Letters 2006; 48(7): 1247-1250.
[15] Su S, Wong K and Tang C. Ultra-wideband square planar antenna for IEEE 802.16a operating in the 2–11 GHz band. Microwave and Optical Technology Letters, 2004; 42 (6): 463-466.
[16] Antonino-Daviu E, Cabedo-Fabres M, Ferrando-Bataller M and Valero-Nogueira A. Wideband double-fed planar monopole antennas. IEE Electronics Letters 2003; 39(23): 1635-1636.
[17] Wong KL, Wu CH and Su SW. Ultrawide-band square planar metal-plate monopole antenna with a trident-shaped feeding strip. Transactions on Antennas and Propagation 2005; 53(4): 1262-1269.
[18] Thomas KG, Lenin N and Sivaramakrishnan R. Ultrawideband planar disc monopole. IEEE Transactions on Antennas and Propagation 2006; 54 (4): 339-1341.
[19] Ammann MJ and Chen ZN. A wide-band shorted planar monopole with bevel. IEEE Transactions on Antennas and Propagation 2003; 51(4): 901- 903.

[20] Wang W, Zhong SS and Liang XL. A broadband CPW-fed arrow-like printed antenna. IEEE Antennas and Propagation International Symposium (Digest), Monterey, CA, Jul. 2004.
[21] Choi SH, Park JK, Kim SK and Park JY. A new ultra-wideband antenna for UWB applications. Microwave and Optical Technology Letters 2004; 40(5): 399 - 401.
[22] Liang JX, Chiau CC, Chen, XD and Parini CG. Study of a printed circular disc monopole antenna for UWB systems. IEEE Transactions on Antennas and Propagation 2005; 53(11): 3500-3504.
[23] Ooi BL, Zhao G, Leong MS, Chua KM and Lu Albert CW. Wideband LTCC CPW-fed two layered monopole antenna. IEE Electronics Letters 2005; 41(16): 889-890.
[24] Lizzi L, Azaro R, Oliveri G and Massa A., Printed UWB antenna operating for multiple mobile wireless standars. IEEE Antennas and Wireless Propagation Letters 2010; 10: 1429-1432.
[25] Kim JP, Yoon TO, *et al.* Design of an ultra wide-band printed monopole antenna using FDTD and genetic algorithm. IEEE Microwave and Wireless Components Letters 2005; 15(6): 395-397.
[26] Low ZN, Cheong JH and Law CL, Low-cost PCB antenna for UWB applications. IEEE Antennas and Wireless Propagation Letters 2005; 4: 237-239.
[27] Osama A, Sebak AR. A printed monopole antenna with two steps and a circular slot for UWB applications. IEEE Antennas and Wireless Propagation Letters 2008; 7: 411-413.
[28] Huang CY and Hsia WC. Planar elliptical antenna for ultra-wideband communications. IEE Electronics Letters 2005; 41(6): 296-297.
[29] Zhang X, Wu W, Yan ZH, Jiang JB and Song Y. Design of CPW-fed monopole UWB antenna with a novel notched ground. Microwave and Optical Technology Letters 2009; 51(1): 88-91.
[30] Azim R., Islam MT and Misran N, Ground modified double-sided printed compact UWB antenna. IEE Electronics Letters 2011; 47(1): 9-11.
[31] Melo DR, Kawakatsu MN, Nascimento DC and Dmitriev V. A planar monopole UWB antennas with rounded patch and ground plane possessing improved impedance matching. Microwave and Optical Technology Letters 2012; 54(2): 335-338.
[32] Liang XL, Zhong SS and Wang W. Tapered CPW-fed printed monopole antenna. Microwave and Optical Technology Letters 2006; 48(7): 1242-1244.
[33] Liang XL, Zhong SS, Wang W and Yao FW. Printed annular monopole antenna for ultra- wideband applications. IEE Electronics Letters 2006; 41(2): 71-72.
[34] Liang XL, Zhong SS and Wang W. UWB printed circular monopole antenna. Microwave and Optical Technology Letters 2006; 48(8): 1532-1534.
[35] Zhong SS and Liang XL. Compact elliptical monopole antenna with impedance bandwidth in excess of 21:1. IEEE Transactions on Antenna Propagation 2007; 55(11): 3082-3085.
[36] Liu JJ, Zhong SS, Esselle KP. A printed elliptical monopole antenna with modified feeding structure for bandwidth enhancement. IEEE Transactions on Antenna and Propagation 2001; 59(2): 667- 670.
[37] Fortino N, Dauvignac JY, Kossiavas G and Staraj R. Design optimization of UWB printed antenna for ominidirectional pulse radiation. IEEE Transactions on Antenna Propagation 2008; 56(7): 1875-1881.

[38] Wu Q, Jin RH, Geng JP and Ding M. Printed omni-directional UWB monopole antenna with very compact size. IEEE Transactions on Antenna and Propagation 2008; 56(3): 896-899.
[39] Sun M, Zhang YP and Lu YL. Miniaturization of planar monopole antenna for ultrawideband radios. IEEE Transactions on Antenna Propagation 2010; 58(7): 2420- 2425.
[40] Jang YW. Broadband cross-shaped microstrip-fed slot antenna. IEE Electronics Letters 2000; 36(25): 2056-2057.
[41] Jang YW, Experimental study of large bandwidth three-offset microstripline-fed slot antenna. IEEE Microwave and Wireless Components Letters 2011; 11(10): 425-427.
[42] Yao FW, Zhong SS and Liang XL. Wideband slot antenna with a novel microstrip feed. Microwave Optical Technology Letters 2005; 46(3): 275-278
[43] Chen HD, Broadband CPW-fed square slot antennas with a widened tuning stub. IEEE Transactions on Antenna Propagation 2003; 51(8): 1982-1986.
[44] Azim R, Islam MT and Misran N. Compact tapered-shape slot antenna for UWB applications. IEEE Antennas and Wireless Propagation Letters 2011; 10: 1190-1193.
[45] Denidni TA and Habib MA. Broadband printed CPW-fed circular slot antenna. IEE Electronics Letters 2006; 42(3): 135-136.
[46] Evangelos SA, Anastopoulos AZ, *et al.* Circular and elliptical CPW-fed slot and microstrip-fed antennas for ultrawideband applications. IEEE Antennas and Wireless Propagation Letters 2006; 5: 294-297.
[47] Chen D and Cheng C H. A novel ultra-wideband microstrip-line fed wide-slot antenna. Microwave and Optical Technology Letters 2006; 48(4): 776-777.
[48] Ghaderi MR and Mohajeri F. A compact hexagonal wide-slot antenna with microstrip - fed monopole for UWB application. IEEE Antennas and Wireless Propagation Letters 2011; 10: 682-685.
[49] Ma TG and Jeng SK. Planar miniature tapered-slot-fed annular slot antennas for ultra-wideband radios. IEEE Transactions on Antenna Propagation 2005; 53(3): 1194- 1202.
[50] Gopikrishna M, Krishna DD, Anandan CK, *et al.* Design of a compact semi-elliptic monopole slot antenna for UWB systems. IEEE Transactions on Antenna Propagation 2009; 57(6): 1834-1837.
[51] Pourahmadazar J, Ghobadi C, Nourinia J, Felegari N and Shirzad H. Broadband CPW-fed circularly polarized squre slot antenna with inverted-L strips for UWB applications. IEEE Antennas and Wireless Propagation Letters 2011; 10: 369-372.
[52] Sim CYD, Chung WT and Lee CH. Compact slot antenna for UWB applications. IEEE Antennas and Wireless Propagation Letters 2010; 9: 63-66.
[53] Liang XL, Denidni TA, Zhang LN, *et al.* Printed binomial- curved slot antennas for various wideband applications. IEEE Transactions on Microwave Theory and Techniques 2011; 59(4): 1058-1065.
[54] Lapierre M, Antar YMM, Ittipiboon A and Petosa A. Ultra wideband monopole/ dielectric resonator antenna. IEEE Microwave and Wireless Components Letters 2005; 15(1): 7-9.
[55] Ruan YF, Guo YX and Shi XQ. Double annular-ring dielectric resonator antenna for ultra-wideband application. Microwave and Optical Technology Letters 2007; 49(2):362-366.

[56] Jazi MN, Denidni TA. Design and implementation of an ultrawideband hybrid skirt monopole dielectric resonator antenna. IEEE Antennas and Wireless propagation Letters 2008; 7: 493-496.
[57] Liang XL, Denidni TA. Cross-T-shaped dielectric resonator antenna for wideband applications. IEE Electronics Letters 2008; 44(2): 1176-1177.
[58] Liang XL, Denidni TA. Wideband L-shaped dielectric resonator antenna with an inverted-trapezoidal patch feed. IEEE Transaction on Antennas and Propagation 2009; 57(1): 272-274.
[59] Zhang LN, Zhong SS and Liang XL. Wideband U-shaped dielectric resonator antenna fed by triangle patch. Microwave and Optical Technology Letters 2010; 52(11): 2435- 2438.
[60] Denidni TA, Weng ZB andmahmoud NJ. Z-shaped dielectric resonator antenna for ultrawideband application. IEEE Transactions On Antennas and Propagation 2010; 58 (12): 4059-4062.
[61] Weng ZB, Wang XM, Jiao YCand Zhang FS. CPW-fed dielectric resonator antenna for ultra-wideband applications. Microwave and Optical Technology Letters 2010; 52(12): 2709- 2712.
[62] Liang XL, Fu X, Jin RH, Geng JP and Ye S. An ultra-wideband dielectric resonator antenna with pattern reconfiguration, International Workshop on Antenna Technology, Hong Kong, China, March, 2011.
[63] Kim Y and Kwon DH. CPW-fed planar ultra wideband antenna having a frequency band notch function. IEE Electronic Letters 2004; 40(7): 403-405.
[64] Chung K, Kim J and Choi J. Wideband microstrip-fed monopole antenna having frequency band-notch function. IEEE Microwave and Wireless Components Letters 2005; 15(11): 766-768.
[65] Zhao YL, Jiao YC, Zhang G, et al. Compact planar monopole UWB antenna with band-notched characteristic. Microwave and Optical Technology Letters 2008; 50(10):2656-2658.Peng L, Ruan CL and Yin XC. Analysis of the small slot-loaded elliptical patch antenna with a band-notched for UWB applications. Microwave and Optical Letters 2009; 51(4): 973-976.
[66] Ojaroudi M, Ghanbari G, Ojaroudi N. and Ghobadi C., Small square monopole antenna for UWB applications with variable frequency band-notch function. IEEE Antennas and Wireless Propagation Letters 2009; 8: 1061-1064.
[67] Jiang JB, Song Y, Yan ZH, Zhang X andWu W. Band-notched UWB printed antenna with an inverted-L-slotted ground. Microwave and Optical Letters 2009; 51(1): 260-263.
[68] Sim CYD, Chung WT and Lee CH. An octagonal UWB antenna with 5GHz band-notch function. Microwave and Optical Letters 2009; 51(1): 74-78.
[69] Tand T, Lin DB, Liou GH and Horng JH, Miniaturized 5.2GHz notched UWB CPW-fed antenna using dual reverse split trapezoid slots. Microwave and Optical Letters 2009; 50(3): 652-655.
[70] Liu L, Yin YZ, Jie C, Xiong JP and Z Cui. A compact printed antenna using slot-type CSRR for 5.2GHz/5.8GHz band-notched UWB application. Microwave and Optical Letters 2008; 50(12): 3239- 3242.

[71] Movahedinia R and Azarmanesh MN. A novel planar UWB monopole antenna with variable frequency band-notch function based on etched slot-type ELC on the patch. Microwave and Optical Letters 2010; 52(1): 229-232.
[72] Jahromi MN, Falahati A and Edwards RM. Application of fractal binary tree slot to design and construct a dual band-notch CPW-ground-fed ultra-wide band antenna, IET Microwave Antennas and Propagation 2011; 5(12):1424-1430.
[73] Lui WJ, Cheng CH, Cheng Y and Zhu H. Frequency notched ultra-wideband microstrip slot antenna with fractal tuning stub. IEE Electronics Letters 2005; 41(6): 294-296.
[74] Chiu CW and Li CS. A CPW-fed band-notched slot antenna for UWB applications. Microwave and Optical Letters 2009; 51(6): 1587-1592.
[75] Cai YL and Feng ZH. A UWB band-notched antenna with novel branches on the back of substrate. Microwave and Optical Letters 2008; 58(12): 3274-3278.
[76] Zhang K, Li YX and Long YL. Band-notched UWB printed monopole antenna with a novel segmented circular patch. IEEE Antennas and Wireless propagation Letters 2010; 9: 1209-1212.
[77] Wu SJ andTarng JH. Planar band-notch ultra-wideband antenna with square-looped and end-coupled resonator. IET Microwave Antennas and Propagation 2011; 5(10): 1227-1233.
[78] Zhang LN, Zhong SS, Liang XL, Du CZ. Compact omnidirectional band-notch ultra-wideband antenna. IEE Electronic Letters 2009; 45(18): 659-660.
[79] Nouri A and Dadashzadeh GR. A compact UWB band-notched printed monopole antenna with defected ground structure. IEEE Antennas and Wireless propagation Letters 2011; 10: 1178-1181.
[80] Yang Y, Yin YZ, Sun AF and Jing SH. Design of a UWB wide-slot antenna with 5.2-/5.8-GHz dual notched bands using modified electromagnetic band-gap structures. Microwave and Optical Letters 2012; 54(4): 1069-1075.
[81] Panda JR and Kshetrimayum RS. 5.5 GHz dual-band notched UWB printed monopole antenna with two open-circuited stubs in the microstrip feedline. Microwave and Optical Letters 2011; 53(12): 2973- 2978.
[82] Abdollahavand M, Dadashzadeh G and Mostaga M. Compact dual band-notched printed monopole antenna for UWB application. IEEE Antennas and Wireless propagation Letters 2009; 9: 1148-1351.
[83] Ye LH and Chu QX. Improved band-notched UWB slot antenna. IEE Electronic Letters 2009; 45(25): 1283-1285.
[84] Zhou ZL, Li L andHong JS. Compact UWB printed monopole antenna with dual narrow band notches for WiMAX/WLAN bands. IEE Electronic Letters 2011; 47(25): 1111-1112.
[85] Niu SF, Gao GP, Li M, Hu YS and Li BN. Design of a novel elliptical monopole UWB antenna with dual band-notched function. Microwave and Optical Letters 2010; 52(6): 1306-1310.
[86] Kim DO and Kim CY. CPW-fed ultra-wideband antenna with triple-band notch function. IEE Electronic Letters 2010; 46(18): 1246-1248.